Int. J. Communications, Network and System Sciences, 2009, 2, 775-785
doi:10.4236/ijcns.2009.28090 Published Online November 2009 (http://www.SciRP.org/journal/ijcns/).

Subcarrier Availability in Downlink OFDM Systems with Imperfect Carrier Synchronization in Deep Fading Noisy Doppler Channels

Litifa NOOR[1], Alagan ANPALAGAN[1], Sithamparanathan KANDEEPAN[2]
[1]*WINCORE Research Lab, Ryerson University, Toronto, Canada*
[2]*Wireless Signal Processing Group, National ICT, Australia*
Email: *alagan@ee.ryerson.ca, lnoor@ee.ryerson.ca*
Received July 11, 2009; *revised August* 30, 2009; *accepted September* 19, 2009

Abstract

Multicarrier systems such as orthogonal frequency division (OFDM) are considered as a promising candidate for wireless networks that support high data rate communication. In this article, we investigate the performance of a multiuser OFDM system under imperfect synchronization. Analytical results indicate that the SNR degrades as the average power of the channel impairments such as AWGN, carrier frequency offset due to Doppler frequency and fading gain is increased. The SNR degradation leads to imperfect synchronization and hence decreases the total number of subcarriers available for allocation. Monte Carlo analysis shows up to 22% loss in the number of allocatable subcarriers can be expected under a specific imperfect synchronization condition as compared to perfect synchronization. We utilize empirical modelling to characterize the available number of subcarriers as a Poisson random variable. In addition, we determine the percentage decrease in the total number of allocatable subcarriers under varying channel parameters. The results indicate 19% decrease in the number of available subcarriers as average AWGN power is increased by 10dB; 44% decrease as the Doppler frequency is varied from 10Hz to 100Hz; and 56% decrease as the fading gain is varied from 0dB to -30dB.

Keywords: OFDM, Subcarrier Availability, Synchronization

1. Introduction

The growing demand for high-speed wireless communications has led to the investigation of spectrally effcient systems for downlink transmission in multicarrier systems [1]. Multicarrier systems such as Orthogonal Frequency Division Multiplexing (OFDM) enable the network to provide high data rate communication by using adaptive subcarrier allocation. Although high data rate communication is subject to inter-symbol interference (ISI) due to dispersive nature of wireless channels, OFDM enables the radio network to support high data rates while reducing the effect of ISI [2,3].

However, OFDM based systems are sensitive to carrier frequency offset (CFO), which leads to the loss of orthogonality between the subcarriers and thus introduction of inter-channel interference (ICI) [4]. CFO is caused by differences in transmitter and receiver oscillator frequencies, Doppler frequency due to relative mobility between transceivers and phase noise introduced by non-linear channels. Since accurate frequency synchronization is very important for reliable signal reception [5], OFDM systems utilize different synchronization schemes to facilitate acquisition and tracking of carrier frequency. However, the distortion inherent in wireless channels requires special design techniques and rather sophisticated adaptive coding and modulation algorithms to achieve accurate synchronization. Different methods have been suggested to reduce the effect of CFO [6–8], but obtaining perfect synchronization in wireless channels remains a challenging task. Hence, in this article we investigate the performance of multiuser OFDM under imperfect synchronization.

In the literature, various subcarrier allocation algorithms have been presented for multiuser OFDM systems. Many of these algorithms support high aggregate data

*This work was supported in part by a grant from National Science and Engineering Research Council of Canada..

rate and maximize system capacity [9–14]. However, the performance improvement is achieved when the system is based on perfect synchronization and the utilization of instantaneous channel information to adaptively allocate subcarriers. Assuming that the channel variation in a frequency selective fading environment is independent of each other, adaptive subcarrier allocation based on instantaneous channel information is an effective method to resource allocation in multiuser OFDM systems. However, obtaining the instantaneous channel condition under hostile wireless channels is not attainable in practical systems. Hence identifying the subcarriers with relatively low SNR and avoiding allocation of such subcarriers is a more practical approach to subcarrier allocation.

In this article, we determine the percentage loss in the available number of subcarriers under imperfect synchronization in comparison to perfect synchronization. The frequency synchronization scheme used is the open-loop maximum likelihood (ML) estimator. The performance of synchronization depends on noise, Doppler frequency and deep-fades in the channel that reduce the effective SNR associated with the subcarrier, which in turn degrades the allocatability of the subcarrier. The purpose of evaluating the system performance under imperfect synchronization is to restrict allocation of the subcarriers that are not suitable for transmission. Although the number of allocatable subcarriers as compared to perfect synchronization decreases which translates to a decrease in the aggregate data rate for a given number of users, the BER performance of the system could be improved by avoiding allocation on subcarrriers that are not suitable for transmission. Hence, any subcarrier allocation algorithm can be utilized while considering the variations in the total number of subcarriers. To the best of our knowledge, this is the first paper to characterize the subcarrier availability in deep fading noisy Doppler channels.

The organization of this article is as follows. In Section 2, the OFDM system model is discussed. In Section 3, we discuss the frequency synchronization utilized for the OFDM system. Following, a detailed analysis of SNR is provided in Section 4. In Section 5, we discuss the number of available subcarriers under imperfect synchronization and model the statistical characteristics of allocatable subcarriers. Following, in Section 6 we evaluate the number of available subcarriers under variable SNR. In Section 7, the paper is concluded.

2. System Model

Figure 1 shows the baseband equivalent model of the OFDM system that is being considered in this paper. This analysis is independent of mapping of the transmitted data as complex values $a_{0,i} \ldots a_{N-1,i}$, and is therefore applicable to all forms of modulation which is utilized in OFDM systems. As indicated in Figure 1, the IFFT is performed on the complex data symbols $a_{k,i}$ for $k = 0, 1, \ldots, N-1$, to produce the time-domain samples $b_{n,i}$ for $n = 0, 1, \ldots, N-1$ as follows:

$$b_{n,i} = \frac{1}{N}\sum_{k=0}^{N-1} a_{k,i} e^{j2\pi(\frac{n}{N})k} \tag{1}$$

where N is the number of data samples. The OFDM symbol $b_{n,i}$ is transmitted through the frequency selective Doppler channel. The frequency response of the channel is indicated by:

$$H_K = \alpha_K e^{j2\pi\frac{k}{N}(\Delta fT)} + \eta_k \tag{2}$$

where α_k is the (Rayleigh) fading gain for the kth subcarrier, $e^{j2\pi\Delta fT}$ is the CFO due to Doppler frequency with Δf indicating the Doppler frequency and T indicating the symbol period, and η_k is the Additive White Gaussian Noise (AWGN) component on the kth subcarrier.

The system is based on the characteristics of multiuser frequency-selective fading channels where different subcarriers are subject to different fading levels and the channel variations in a multiuser environment are independent of each other. To ensure frequency selectivity, the coherence bandwidth of the channel, which is the reciprocal of the multi-path spread, is assumed to be smaller in comparison to the bandwidth of the transmitted signal.

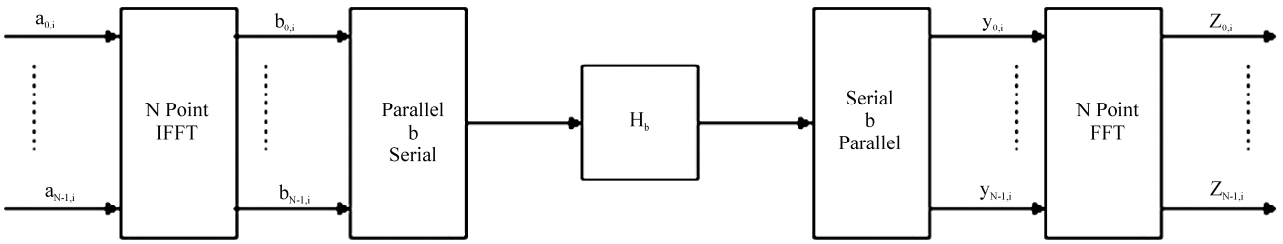

Figure 1. Baseband Equivalent OFDM System Model.

Under the assumption of AWGN channel, the received signal with the frequency offset and the fading gain is given as:

$$\begin{aligned} y_k &= \sum_{n=0}^{N-1} \alpha_k a_k e^{j2\pi(\frac{n}{N})k} e^{j2\pi(\frac{\Delta fT}{N})k} + \eta_k \\ &= \sum_{n=0}^{N-1} \alpha_k a_k e^{j2\pi(\frac{n}{N}+\frac{\Delta fT}{N})k} + \eta_k \end{aligned} \tag{3}$$

The received signal on the *kth* subcarrier and in the *ith* symbol period can be written as:

$$y_{k,i} = a_{k,i}\alpha_{k,i} e^{j2\pi N(\Delta fT)} + \eta_k \ , \tag{4}$$

where $a_{k,i}$ is the transmitted data on the *kth* subcarrier in the *ith* symbol period, and $\Delta f\ T$ is the normalized frequency offset.

The received signal after FFT is expressed as:

$$\begin{aligned} z_{m,i} &= \sum_{k=o}^{N-1} y_{k,i} e^{-j2\pi\frac{km}{N}} + \eta_m \\ &= \frac{1}{N}\sum_{l=o}^{N-1} \alpha_{l,i} a_{l,i} \sum_{k=0}^{N-1} e^{j2\pi\frac{k}{N}(l-m+\Delta fT)} + \eta_m \end{aligned} \tag{5}$$

Using the properties of geometric series, $z_{m,i}$ can be expressed as:

$$z_{m,i} = \frac{1}{N}\sum_{l=0}^{N-1} \alpha_{l,i} a_{l,i} \frac{\sin\pi(l-m+\Delta fT)}{\sin\frac{\pi}{N}(l-m+\Delta fT)} e^{j\frac{N-1}{N}(l-m+\Delta fT)} + \eta_m \tag{6}$$

The analysis of ICI can be simplified by defining N complex weighting coefficients, c_0, ..., c_{N-1}, which give the contribution of each of the N point values $a_{0,I}$, ...$a_{N-1,i}$ to the output value. Based on this, $z_{m,i}$ is written as:

$$z_{m,i} = c_o \alpha_{m,i} a_{m,i} + \sum_{l=0,l\neq m}^{N-1} c_{l-m} \alpha_{l,i} a_{l,i} + \eta_m \tag{7}$$

where the first term is the desired signal and second term is the ICI. c_o is the attenuation factor, $a_{m,i}$ is the transmitted data on the *mth* subcarrier in the *ith* symbol period, and $\alpha_{m,i}$ is the (Rayleigh) fading gain on the *mth* subcarrier during *ith* symbol period.

Using geometric series expansion, $z_{m,i}$ can be written as:

$$z_{m,i} = \frac{1}{N}\frac{\sin\pi(\Delta fT)}{\sin\frac{\pi}{N}(\Delta fT)} e^{j\pi(\frac{N-1}{N})(\Delta fT)} \alpha_{m,i} a_{m,i} + \sum_{l=0,l\neq m}^{N-l} \frac{1}{N}\frac{\sin\pi(l-m+\Delta fT)}{\sin\frac{\pi}{N}(l-m+\Delta fT)} \times \alpha_{l,i} a_{l,i} e^{j\pi(\frac{N-1}{N})(l-m+\Delta fT)} + \eta_m \tag{8}$$

For noiseless case, when $\Delta f\ T = 0$, $z_{m,i} = a_{m,i} + \eta_m$ which indicates the transmitted data plus noise. In the case where $\Delta f \neq 0$, the transmitted data is subject to attenuation and ICI.

In addition, the relationship between the attenuation component $c0$ and $\Delta f\ T$ indicates that attenuation in the desired signal component increases as the $\Delta f\ T$ is increased. Given that an increase in CFO is caused by an increase in the Doppler frequency, it can be seen that as the Doppler frequency is increased the attenuation in the desired signal increases leading to a decrease in the SNR.

The $\alpha_{m,i}$ is the (Rayleigh) fading gain for the *mth* subcarrier in the *ith* symbol period which attenuates the desired signal, which in turn reduces the SNR. Each subcarrier experiences a different level of fading and the maximum number of subcarriers that are in deep fade are dependent on the channel condition and vary every transmission time. The deep-fading in the channel degrades the corresponding subcarriers by reducing the effective SNR associated with the subcarrier.

3. Frequency Synchronization

To emulate imperfect synchronization, the system is considered under channel impairments such as Doppler frequency and frequency selective fading. The Doppler frequency leads to substantial CFO and the frequency selective fading subjects the subcarriers to independent fading gains. The CFO and the deep-fades in the channel degrade the corresponding subcarriers which reduces the effective SNR associated with the subcarrier. This makes the synchronization system at the receiver to perform poorly, and eventually lose lock with the corresponding subcarriers. Hence, the system experiences imperfect synchronization.

The frequency synchronization scheme utilized for the OFDM system is the well-known open-loop maximum likelihood (ML) estimator [15–17]. The frequency estimator gives rise to some jitter in the estimated frequency, increasing with decreasing SNR, due to the input noise. Correspondingly, the symbol error probability performance also degrades due to imperfect carrier recovery at low SNR. To avoid this, we set a threshold limit on the synchronizer, making sure that the frequency jitter does not exceed a certain limit. The frequency jitter has to be less or equal to the threshold frequency for the subcarrier to be declared as available for allocation. In this work, the threshold frequency is set as 10Hz. If the synchronizer is unable to lock to the carrier with this threshold limit, due to noise, Doppler frequency or deep fades, then we declare the subcarrier to be un-lockable during the given transmission time. Hence, the subcarrier is declared as not suitable for allocation.

Under the assumption of constant received signal power, as the noise power increases the number of sub-

carriers available for transmission decreases. The decrease in the total number of subcarriers available for reliable transmission imposes limitation on the total achievable data rate by the system. Hence, determining the decrease in the number of available subcarriers under imperfect synchronization which is the case in practical systems is important in assessing the accurate system performance.

4. SNR Analysis

In this section, we derive the expression for the SNR on the *mth* subcarrier as:

$$SNR_m = \frac{p_{D_m}}{P_{I_m} + P_{N_m}} \tag{9}$$

where P_{Dm} is the average power of the desired signal, P_{Im} is the average interference power and P_{Nm} is the average noise power on the *mth* subcarrier. The average power of the desired, interference and noise on the *mth* subcarrier is defined as

$P_{D_M} = E\left[\left|D_m\right|^2\right], P_{I_m} = E\left[\left|N_m\right|^2\right]$, and $P_{N_m} = E\left[\left|N_m\right|^2\right]$

respectively. Hence, the average SNR on the *mth* subcarrier is formulated as:

$$SNR_m = \frac{E\left[\left|D_m\right|^2\right]}{E\left[\left|I_m\right|^2\right] + E\left[\left|N_m\right|^2\right]} \tag{10}$$

where the average power of the desired signal is calculated as:

$$E\left[\left|D_m\right|^2\right] = E\left[\left|c_o \alpha_{m,i} a_{m,i}\right|^2\right] \tag{11}$$

Assuming that the transmitted data and the fading gain are independent, the average power of the desired signal can be written as:

$$E\left[\left|D_m\right|^2\right] = \left|c_o\right|^2 E\left[(\alpha_{m,i})^2\right] E\left[(\alpha_{m,i})^2\right] \tag{12}$$

The ICI power is expressed as:

$$\begin{aligned} E\left[\left|I_m\right|^2\right] &= E\left[\left|\sum_{l=0, l\neq m}^{N-1} c_{l-m}\alpha_{l,i} a_{l,i}\right|^2\right] \\ &= \sum_{l=0, l\neq m}^{N-1} \left|c_{l-m}\right|^2 E\left[\left(\alpha_{l,i}\right)^2\right] E\left[\left(a_{l,i}\right)^2\right] \end{aligned} \tag{13}$$

The above equation can be simplified as [4]:

$$E\left[\left|I_m\right|^2\right] = \left(1 - \left|c_o\right|^2\right) E\left[\left(\alpha_{l,i}\right)^2\right] E\left[\left(a_{m,i}\right)^2\right] \tag{14}$$

The power of the noise is expressed as :

$$E\left[\left|N_m\right|^2\right] = No \tag{15}$$

Hence, the SNR on the *mth* subcarrier is written as:

$$SNR_m = \frac{\left|c_o\right|^2 E\left[(\alpha_{m,i})^2\right] E\left[(a_{m,i})^2\right]}{(1 - \left|c_o\right|^2) E\left[(\alpha_{l,i})^2\right] E\left[(a_{m,i})^2\right] + N_o} \tag{16}$$

The above equation indicates the dependence of the SNR on the noise, frequency offset due to Doppler frequency and fading gain. Hence, as the average noise power increase the SNR decreases. In addition, to show the dependence of SNR on the CFO due to Doppler frequency, we express c_o as a function of $\Delta f\ T$. Hence, the SNR is written as:

$$SNR_m = \frac{\varnothing(\Delta fT) E\left[(\alpha_{m,i})^2\right] E\left[(a_{m,i})^2\right]}{(1 - \varnothing(\Delta fT)) E\left[(\alpha_{l,i})^2\right] E\left[(a_{m,i})^2\right] + N_o} \tag{17}$$

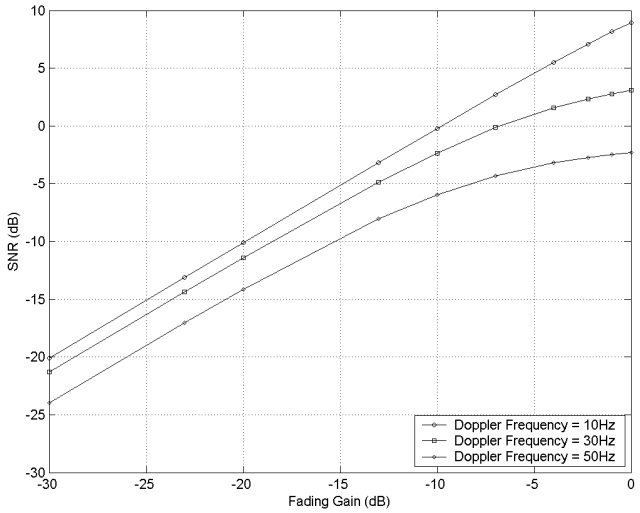

Figure 2. SNR versus Fading gain with different Doppler Frequency and constant average noise power of -10dB.

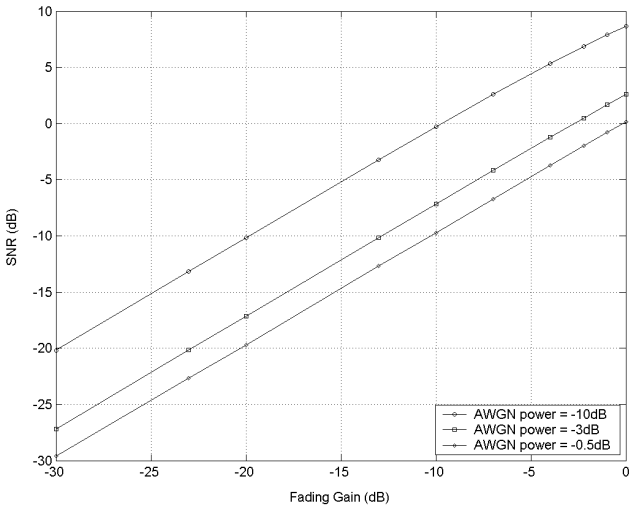

Figure 3. SNR versus Fading gain with different AWGN power and constant Doppler Frequency of 10Hz.

This expression clearly indicates that the desired signal and interfering power decrease due to CFO which in turn causes the SNR to decrease.

Analysis is performed to study the changes in the SNR as the average power of channel parameters such as average noise power, Doppler frequency and fading gain are varied.

Figure 2 indicates the changes in the SNR as the average fading gain is varied between -30dB to 0dB when average noise power is kept constant at -10dB. The SNR performance is evaluated under Doppler frequency of 10Hz, 30Hz, and 50Hz. As evident from (17), the average power of the fading gain degrades the signal power as well as the interference power. Hence, the increase in the average power of the fading gain degrades the SNR as indicated in Figure 2. Also, the increase in the Doppler frequency causes the interference power to increase. It is evident from this figure that as the Doppler frequency increases, the SNR decreases. The increase in the Doppler frequency from 10Hz to 50Hz results in 12dB decrease in the SNR for an average fading gain of 0dB.

Figure 3 indicates the changes in the SNR as the average fading gain is varied between -30dB to 0dB and the Doppler frequency is kept at 10Hz. The SNR performance is evaluated under average noise power of -10dB, -3dB and -0.5dB. As evident from (17), the increase in the average noise power increases the noise power and hence degrades the SNR. As illustrated in Fig. 3, when the average noise power is increased by 9.5dB, the SNR decreases by 9dB for an average fading gain of 0dB.

To maintain the adaptivity of the system further simplifying of (17) is avoided. Instead, Monte Carlo analysis is performed with values generated from Rayleigh distributions. Due to random nature of time variant multipath channels, it is reasonable to characterize such channels statistically. The random variable α_m is usually modelled using Rayleigh distribution and the subcarriers that are in deep-fade are not utilized during any transmission time interval in our case. To analyze the random effect, Monte Carlo analysis is performed to obtain the characteristics of the channel. Although the fading gains follow Rayleigh distribution, only the subcarriers that are identified as allocatable by the ML threshold limit are declared as allocatable.

5. Available Subcarriers with Imperfect Synchronization

In this section, an analysis is performed to quantify the variations in the number of available subcarriers under imperfect synchronization which results from noise, Doppler shift and frequency selective fades in the channel.

To emulate the effect of imperfect synchronization in a multiuser OFDM system, the average noise power, Doppler frequency and average fading level are selected as −3dB, 25Hz and −4dB respectively. The threshold frequency is set as 10Hz. The carrier frequency of the system is selected to be 4GHz and the forward link channel bandwidth is 20MHz. The total number of subcarriers, N, is 64 and the subcarrier bandwidth is 312.5kHz. The objective of the simulation is to obtain the average number of subcarriers for each user under imperfect synchronization and the variations in the total available subcarriers as the number of users is varied.

5.1. Number of Available Subcarriers under Constant SNR

The simulation results indicate that the number of subcarriers available for users varies in each transmission

time slot and under imperfect synchronization the total number of subcarriers available for reliable transmission is smaller compared to perfect synchronization. The availability of subcarriers for a certain user can be defined as follows:

$$N_a^k = N_T^K - N_{\bar{a}}^k \tag{18}$$

where N_a^k is the number of available subcarriers, N_T^K is the total number of subcarriers and $N_{\bar{a}}^k$ is the number of subcarriers that are not suitable for allocation for the *kth* user. The $N_{\bar{a}}^k$ varies for different users supporting the fact that the channel conditions in a multipath environment is random and changes for each user.

Under the specified channel conditions, in a multiuser environment the average number of subcarriers available for User-1 is 49 and for User-2 is 48. This translates to 77% and 75% available subcarriers for User-1 and User-2 respectively in comparison to perfect synchronization. To ensure reliable data trans mission, subcarrier allocation algorithms should consider the variations in the total available subcarriers for each user and avoid allocating subcarriers from $N_{\bar{a}}^k$.

In addition, we determine the maximum and minimum number of available subcarriers under a given SNR in a multiuser environment. As indicated in Figure 4, as the number of users increase, the minimum number of available subcarriers for transmission decreases while the maximum number of subcarriers available for transmission increases. This indicates that over a large number of trials the average number of allocatable subcarrier is 46.

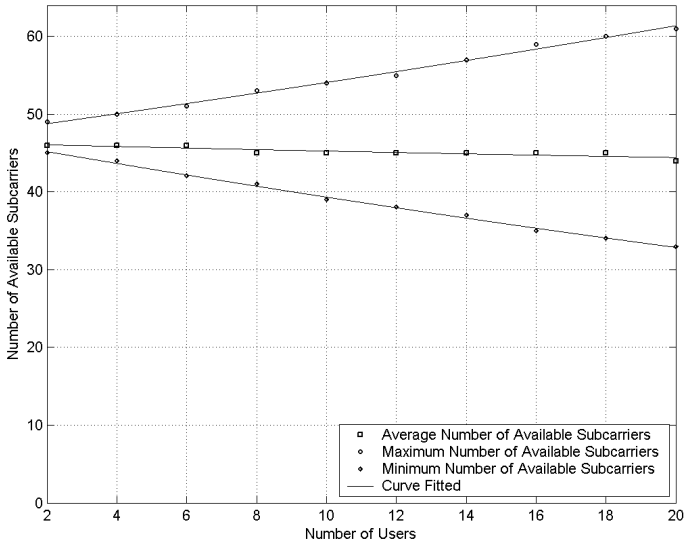

Figure 4. Number of available subcarriers versus number of users.

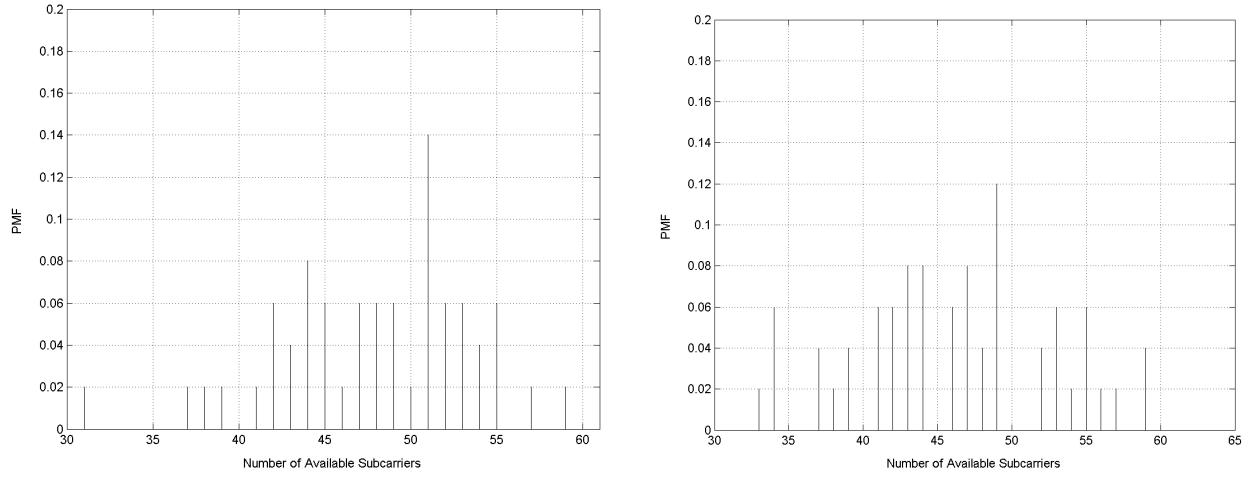

(a) User-1 (b) User-2

Figure 5. Probability mass function of the available subcarriers.

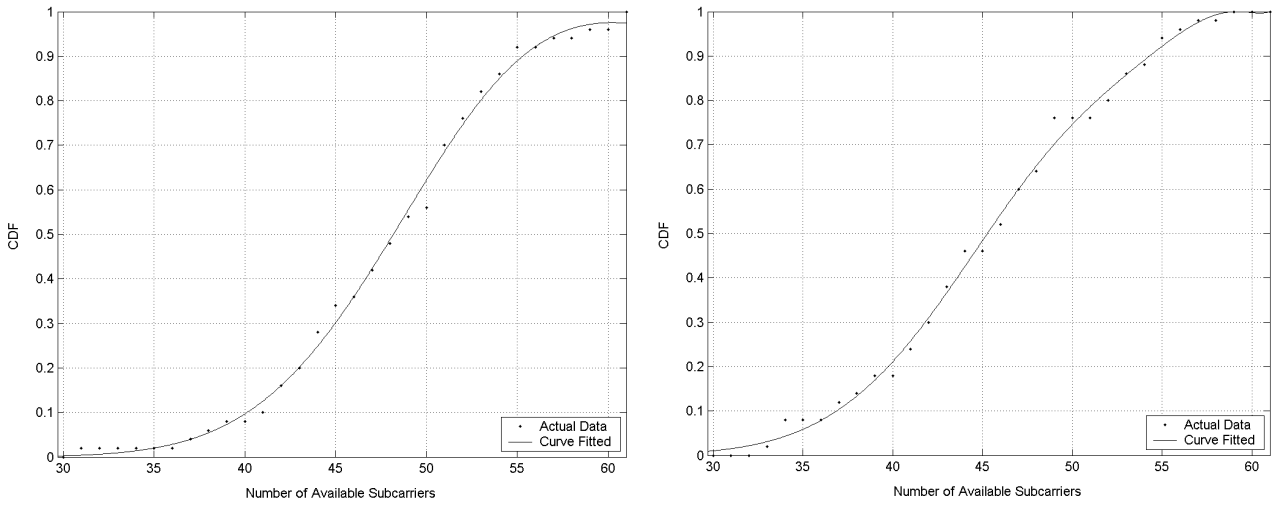

(a) User-1 (b) User-2

Figure 6. Cumulative distribution function of the available subcarriers.

In addition, the maximum and minimum available subcarriers indicate the upper and lower bound of the achievable data rate for the users since the data rate is directly proportional to available subcarriers. It can be stated that while the average available subcarriers does not vary significantly with the increase in the number of users, the minimum and maximum available subcarriers indicate noticeable variations. As the number of users increases, the difference between the maximum and minimum available subcarrier increases, which provides flexibility in the total number of allocatable subcarriers. This system characteristic supports multiplexing gain which in turn increases the aggregate data rate.

5.2. Statistical Model of the Subcarrier Availability

In this section, empirical analysis is used to determine the statistical characteristics of the number of available subcarriers. Given that the number of available subcarriers for transmission is a random variable that takes countable values, it is modelled as a discrete random variable (DRV) [18]. The obtained results are used to develop the probability mass function (PMF) of the available subcarriers for User-1 and User-2, which is indicated in Figure 5. The PMFs are used to obtain the cumulative distribution function (CDF) for both users which is given in Figure 6.

Based on the PMF of the number of available subcarriers, it is identified as a Poisson random variable (PRV) with the parameter λ that defines the average number of available subcarriers in a given time interval.

In our simulation, it is observed that λ for User-1 and User-2 are 51 and 49 respectively. In general, for all users λ is the same on average and hence the number of allocatable subcarriers is a PRV.

The DRV is identified as a PRV because it has the characteristics of a PRV which are explained bellow:

1) The number of available subcarriers is determined in transmission time slot with a fixed length, t_s.

2) The number of available subcarriers for each user varies in the time interval t_s but over a time period of Nt_s the number of available subcarriers for each user has a constant average.

3) The number of subcarriers that are available in disjoint time intervals are statistically independent because the fading gains are uncorrelated.

Although the number of available subcarriers is a PRV, the availability of each subcarrier for trans- mission can be modelled as a Bernoulli random variable (BRV) where the availability of the each is indicated by a 0 indicating not available for allocation and 1 available for allocation. Each subcarrier availability can be viewed as a Bernoulli trial because the number of available subcarrier in each trial is independent, and at most a certain number of subcarriers is determined in each trial. This further supports modelling of the total number of available subcarrier as a PRV since a sequence of Bernoulli trials occurring in time is modelled as a PRV.

Based on the above observations, the number of available subcarriers is identified as a PRV with mean, $\lambda = 0.78N$, where N is the total number of subcarriers. Hence, the average percentage loss of the subcarriers under imperfect synchronization is 22% under the specified channel condition.

To avoid performance degradation in terms of subcarrier availability for transmission, perfect synchronization is required. Since practical systems are subject to imperfect synchronization, the analysis indicates that determining the availability of subcarriers for transmission is essential in the optimization process of radio resource allocation for multiuser systems.

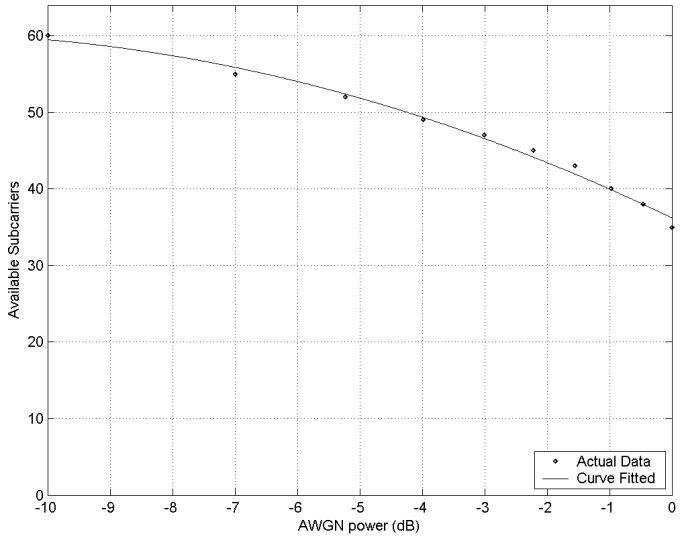

Figure 7. Number of available subcarriers versus AWGN power.

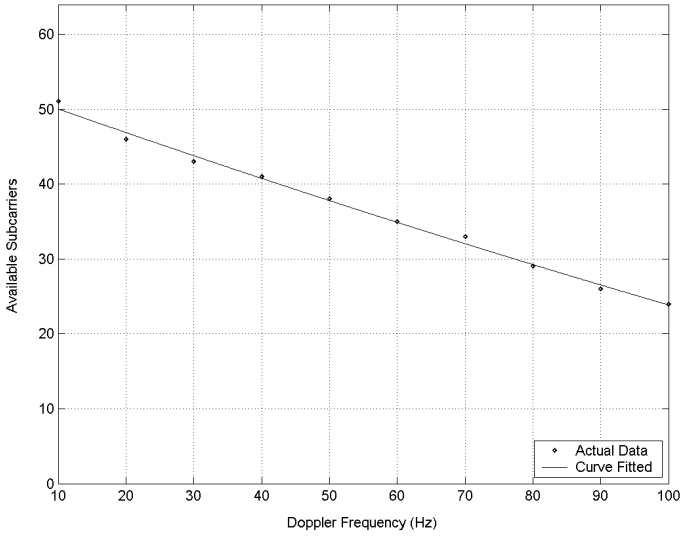

Figure 8. Number of available subcarriers versus Doppler Frequency.

6. Number of Available Subcarriers under Variable SNR

In this section, we investigate the variations in the total number of subcarriers as the factors such as, average noise power, which is modelled as AWGN, Doppler frequency, and fading gain are changed.

6.1. AWGN

To determine the changes in the number of available subcarriers, the AWGN power is varied while the Doppler frequency and the fading gain are kept constant at values of 25Hz and −4dB respectively. Figure 7 shows the number of available subcarriers under different AWGN power. Based on the results, as the AWGN power is varied between −10dB to 0dB, the number of available subcarriers decreases by 19%.

6.2. Doppler Frequency

To investigate the variations in the number of available subcarriers as the Doppler frequency is changed while the AWGN power and the fading gain are kept constant at values of −3dB and −4dB respectively. As illustrated in Figure 8, as the Doppler frequency is varied between 10Hz to 100Hz the number of available subcarriers decreases by 44%.

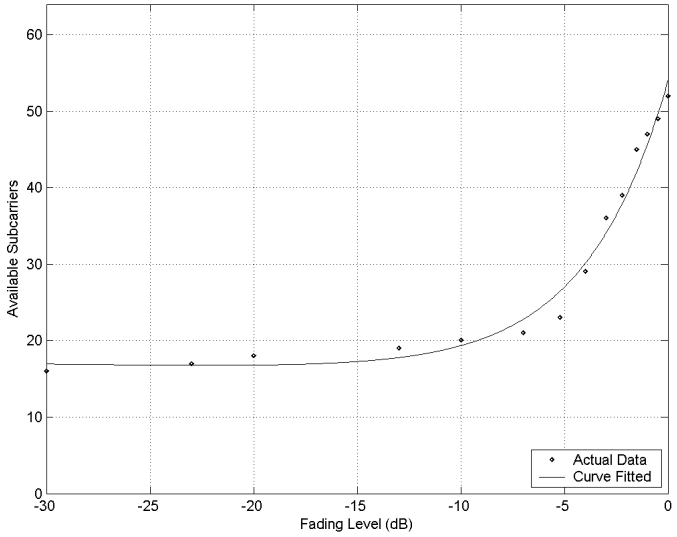

Figure 9. Number of available subcarriers versus fading level.

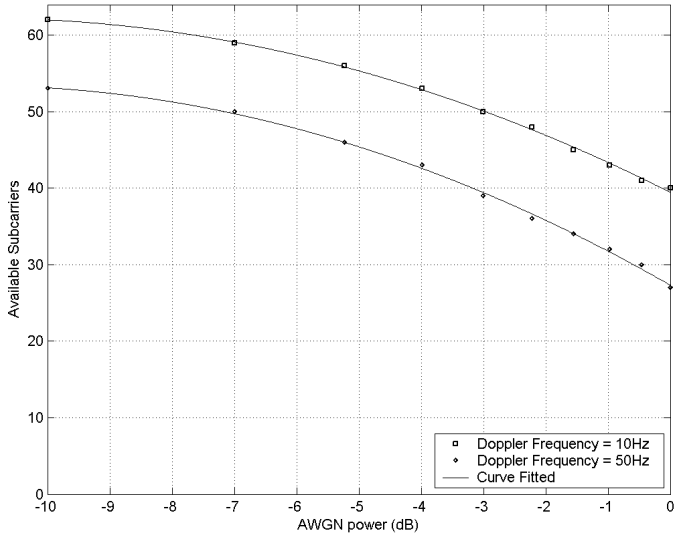

Figure 10. Number of available subcarriers versus AWGN power for different Doppler Frequency.

6.3. Frequency Selective Fading

To determine the changes in the number of available subcarriers as the fading level is varied, the AWGN power and the Doppler frequency are kept constant at −3dB and 25Hz respectively. Figure 9 depicts the corresponding number of subcarriers as the fading level is varied between −30 to 0dB. Hence, as the fading level is varied between 0dB to −30dB the number of available subcarries decreases by 56%.

To further analyze the effect of the hostile channel conditions such as AWGN power, deep-fading and Doppler frequency, the number of available subcarriers is determined with the variation in both the AWGN power and the Doppler frequency under a constant fading gain of −4dB. Figure 10 shows the number of available subcarriers with the variations in AWGN power and Doppler frequency. Based on the results, it can be stated that 40Hz increase in the Doppler frequency leads to 20% decrease in the number of available subcarriers for an AWGN power of 0dB.

In addition, the number of available subcarriers is determined with the variation in both the AWGN power and the fading level under a constant Doppler frequency of 25Hz. Figure 11 shows the number of available subcarriers with the variations in AWGN power and fading levels. As evident from this figure, 20dB increase in fading gain results in 12% decrease in the number of available subcarriers for an AWGN power of 0dB.

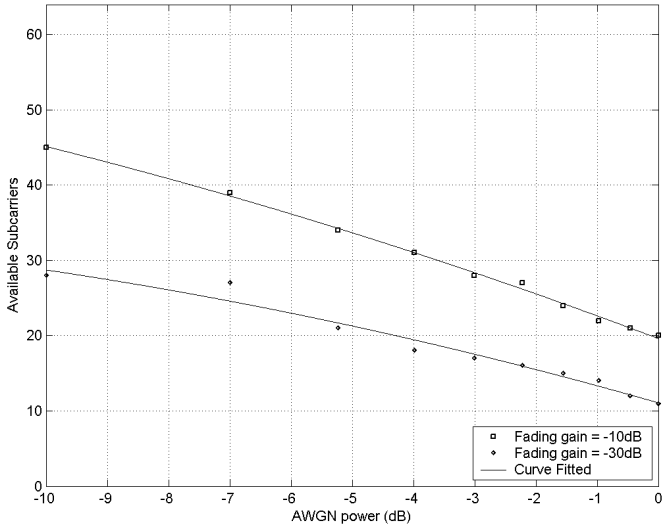

Figure 11. Number of available subcarriers versus AWGN power for different fading gain.

Hence, channel constraints such as AWGN, Doppler effect and frequency selective fading impose noticeable implication on system performance. The total number of available subcarriers changes with the variation in the AWGN power, Doppler shift and fading level. Thus, under imperfect synchronization, which is the case in most communication systems, not all the subcarriers are available for transmission.

7. Conclusions

To avoid performance degradation in terms of subcarrier availability for transmission, perfect synchronization is required. Since practical systems are subject to imperfect synchronization, the analysis indicates that determining the availability of subcarriers for transmission is essential in the optimization process of radio resource allocation. In this paper, we perform an analysis to determine the SNR degrades as the average power of the channel impairments such as AWGN, CFO due to Doppler frequency and fading gain are increased. The decrease in SNR causes imperfect synchronization and hence reduces the total number of available subcarriers for allocation. We use empirical modelling to characterize the number of available subcarriers as Poisson random variable and it is determined that under imperfect synchronization up to 22% of the subcarriers are not suitable for transmission as compared to perfect synchronization under certain channel conditions. We have determined the variations in the number of available subcarriers with the changes in the parameters such as AWGN, Doppler frequency and deep fades that introduce imperfect synchronization. It has been illustrated that a 10dB increase in the average AWGN power leads to 19% decrease in the total number of allocatable subcarriers; a variation of 10Hz to 100Hz in Doppler frequency causes 44% decrease in the number of allocatable subcarriers, and changes in the fading level between 0dB to −30dB result in 56% decrease in the number of allocatable subcarriers. Thus, under imperfect synchronization all the subcarriers are not available for transmission. Given that the data rate is directly proportional to the total number of available subcarriers for transmission, to provide a realistic measure of the system capacity subcarrier allocation algorithms should be based on the number of avail- able subcarriers under imperfect synchronization. Although subcarrier allocation under the constraint of imperfect synchronization does not support more users or higher data rates, it improves system reliability by eliminating allocation on unavailable subcarriers and hence improving the system BER performance.

8. References

[1] D. H. J. Sun and J. SauVola, "Features in future: 4g visions from a technical perspective," IEEE GLOCOM, Vol. 6, pp. 3533–3537, November 2001.

[2] L. J. Cimini, "Analysis and simulation of a digital mobile channel using orthogonal frequency division multiplexing," IEEE Transaction on Communications, pp. 665–675, July 1995.

[3] J. A. C. Bingham, "Multicarrier modulation for data transmission: An idea whose time has come," IEEE Communication Magazine, pp. 5–14, 1990.

[4] M. v. B. T. Pollet and M. Moeneclaey, "Ber sensitivity of ofdm systems to carrier frequency offset and wiener phase noise," IEEE Transaction on Communications, Vol. 43, pp. 191–193, 1995.

[5] M. Luise and R. Reggiannini, "Carrier frequency acquisition and tracking for OFDM systems," IEEE Transaction

on Communications, Vol. 44, 1996.

[6] P. H. Moose, "A technique for orthogonal frequency division multiplexing frequency offset correction," IEEE Transaction on Communications, Vol. 42, pp. 2908–2913, 1994.

[7] P. B. J. van de Beek and M. Sandell, "Ml estimation of timing and frequency offset in ofdm systems," IEEE Transaction on Signal Procesings, Vol. 45, pp. 1800–1805, 1997.

[8] S. K. N. Lashkarian, "Globally optimum ml estimation of timing and frequency offset in ofdm systems," IEEE International Conference on Communications, Vol. 2, pp. 1044–1048, 2000.

[9] K. L. R. M. C. Y. Wong, and R. S. Cheng, "Multiuser OFDM with adaptive subcarrier, bit, and power allocation," IEEE Journal, Selected Areas in Communications, Vol. 17, 1999.

[10] J. Jang and K. B. Lee, "Transmit power adaptation for multiuser OFDM systems," IEEE Journal, Selected Areas in Communications, Vol. 21, 2003.

[11] B. E. Z. Shen and J. G. Andrews, "Optimal power allocation in multiuser OFDM systems," IEEE Global Telecommunications Conference, Vol. 1, 2003.

[12] J. C. W. Rhee, "Increased in capacity of multiuser ofdm system using dynamic subchannel allocation," IEEE 51st, Vehicular Technology Conference, Vol. 2, 2000.

[13] S. Y. C. Suh and Y. Cho, "Dynamic subchannel and bit allocation in multiuser OFDM with a priority user," IEEE Eighth International Symposium, Spread Spectrum Techniques and Applications, pp. 919–923, 2004.

[14] P. Song and L. Cai, "Multi-user subcarrier allocation with minimum rate request for downlink OFDM packet transmission," IEEE 59th Vehicular Technology Conference, Vol. 4, 2004.

[15] D. Rife and R. Boostyn, "Single-tone parameter estimation from discrete-time observations," IEEE Transaction on Information Theory, Vol. 5, 1974.

[16] S. Kandeepan, "Synchronisation techniques for digital modems," PhD thesis, University of Technology, Sydney, July 2003.

[17] S. Kandeepan and S. Reisenfeld, "Performance analysis of a correlator based maximum likelihood frequency estimator," SPCOM, pp. 169–173, 2004.

[18] S. Ross, "Introduction to probability models," Academic Press, 2003.

